Received: 28 September 2019 | Revised: 13 January 2020 | Accepted: 16 January 2020

DOI: 10.1002/bit.27276

BIOTECHNOLOGY BIOENGINEERING WILEY

ARTICLE

# High-level heterologous production of propionate in engineered *Escherichia coli*

Dragan Miscevic[1] | Ju-Yi Mao[2] | Murray Moo-Young[1] | Chih-Hsiung Perry Chou[1]

[1]Department of Chemical Engineering, University of Waterloo, Waterloo, Ontario, Canada

[2]Department of Bioscience and Biotechnology, National Taiwan Ocean University, Keelung, Taiwan

**Correspondence**
Chih-Hsiung (Perry) Chou, Department of Chemical Engineering, University of Waterloo, 200 University Avenue West, Waterloo, ON N2L 3G1, Canada.
Email: cpchou@uwaterloo.ca

**Funding information**
Networks of Centers of Excellence of Canada, Grant/Award Number: BioFuelNet Canada (BFN); Natural Sciences and Engineering Research Council of Canada, Grant/Award Numbers: Canada Research Chair (CRC) grant 950-211471, Strategic Partnership grant 430106-12

## Abstract

A propanologenic (i.e., 1-propanol-producing) bacterium *Escherichia coli* strain was previously derived by activating the genomic sleeping beauty mutase (Sbm) operon. The activated Sbm pathway branches out of the tricarboxylic acid (TCA) cycle at the succinyl-CoA node to form propionyl-CoA and its derived metabolites of 1-propanol and propionate. In this study, we targeted several TCA cycle genes encoding enzymes near the succinyl-CoA node for genetic manipulation to identify the individual contribution of the carbon flux into the Sbm pathway from the three TCA metabolic routes, that is, oxidative TCA cycle, reductive TCA branch, and glyoxylate shunt. For the control strain CPC-Sbm, in which propionate biosynthesis occurred under relatively anaerobic conditions, the carbon flux into the Sbm pathway was primarily derived from the reductive TCA branch, and both succinate availability and the SucCD-mediated interconversion of succinate/succinyl-CoA were critical for such carbon flux redirection. Although the oxidative TCA cycle normally had a minimal contribution to the carbon flux redirection, the glyoxylate shunt could be an alternative and effective carbon flux contributor under aerobic conditions. With mechanistic understanding of such carbon flux redirection, metabolic strategies based on blocking the oxidative TCA cycle (via Δ*sdhA* mutation) and deregulating the glyoxylate shunt (via Δ*iclR* mutation) were developed to enhance the carbon flux redirection and therefore propionate biosynthesis, achieving a high propionate titer of 30.9 g/L with an overall propionate yield of 49.7% upon fed-batch cultivation of the double mutant strain CPC-SbmΔ*sdhA*Δ*iclR* under aerobic conditions. The results also suggest that the Sbm pathway could be metabolically active under both aerobic and anaerobic conditions.

KEYWORDS

*Escherichia coli*, glycerol, propionate, propionyl-CoA, sleeping beauty mutase, TCA cycle

## 1 | INTRODUCTION

Growing socioeconomic and environmental concerns over petro-based chemical products and their production processes have sparked a wide range of technological interests in bio-based production from renewable resources. With rapid biotechnological advances, particularly in synthetic biology, systems biology, genetic engineering, metabolic engineering, and bioinformatics, and so forth, considerable strategies have been developed over the past decades to customize microbial cell factories for bio-based production (Cho, Choi, Luo, & Lee, 2015). Consequently, a number of bio-based commodity products (Fabbri et al., 2018) have been made on industrial scales, such as organic acids (Show et al., 2015), amino acids (Ikeda, 2003), and biodegradable polymers (Chen, 2009).

Propionate, the anion of propionic acid, is a three-carbon carboxylic acid with a wide array of applications in the food (as a preservative, additive, or flavoring agent) and chemical (as an intermediate for chemical synthesis of herbicides, pharmaceuticals, dyes, textile and rubber products, plastics, plasticizers, cosmetics, and perfumes) industries. Although industrial production of propionate has long been carried out by chemical hydrocarboxylation of ethylene or oxidation of propionaldehyde for decades, various biotechnological production methods have also been proposed (Ahmadi, Khosravi-Darani, & Mortazavian, 2017). Thus far, microbial production of propionate is conducted using natural producers of anaerobic Propionibaterium spp., such as *Propionibacterium freudenreichii*, *Propionibacterium acidipropionici*, and *Propionibacterium shermanii*. In spite of high propionate-producing capacity, this genus can suffer various technological limitations, such as low growth rates, use of costly/complex growth media, lack of genetic amenability, and byproduct formation complicating downstream processing (Gonzalez-Garcia et al., 2017). As a result, the use of genetically tractable bacterium *Escherichia coli* as a host for heterologous production of propionate has been proposed (Akawi, Srirangan, Liu, Moo-Young, & Chou, 2015).

Natural *E. coli* produces neither propionate nor its precursor propionyl-CoA. Hence, we derived a propanologenic (i.e., 1-propanol-producing) *E. coli* strain by activating the genomic sleeping beauty mutase (Sbm) operon (Srirangan et al., 2013, 2014). The Sbm operon consists of four genes, that is, *sbm–ygfD–ygfG–ygfH*, and the encoding enzymes are involved in extended dissimilation of succinate for fermentative production of 1-propanol and propionate with propionyl-CoA as a metabolic hub (Figure 1). Using this propanologenic *E. coli* strain, we demonstrated biosynthesis of 1-propanol (Srirangan et al., 2014) and propionate (Akawi et al., 2015) from "unrelated" carbons, such as glucose and glycerol. As the nonnative propionyl-CoA exists in this propanologenic *E. coli* strain, we further implemented relevant synthetic pathways for heterologous production of various propionyl-CoA-derived chemicals, including butanone (Srirangan, Liu, Akawi et al., 2016) and

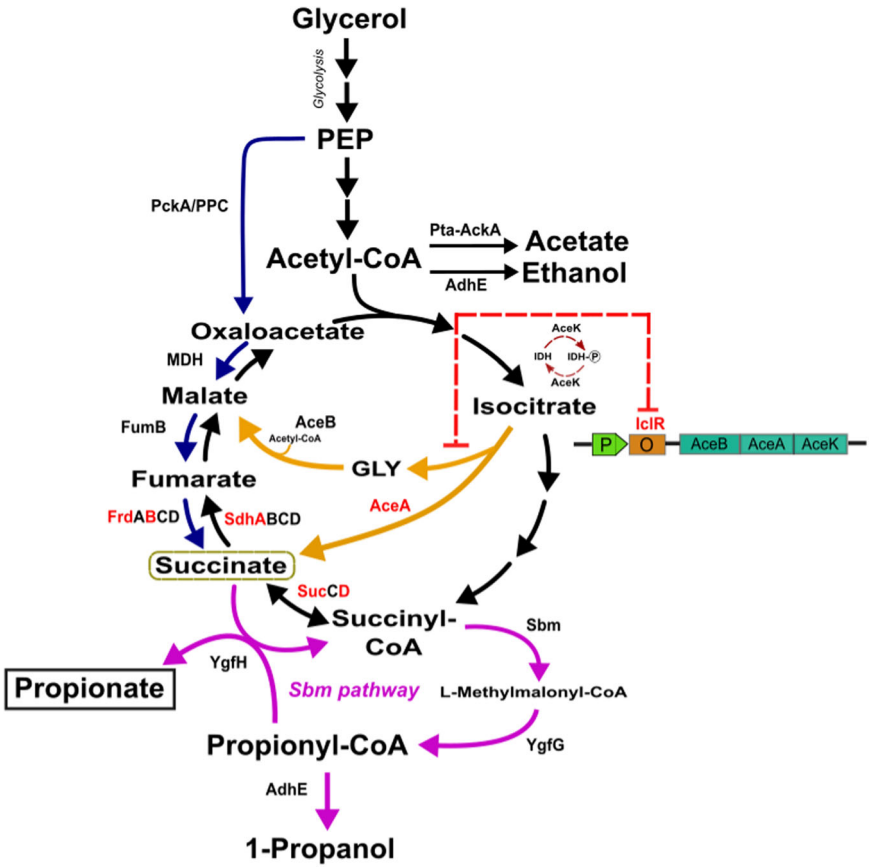


**FIGURE 1** Schematic representation of the engineered propionate production pathway in *Escherichia coli* from glycerol. Metabolic pathways outlined: glycerol dissimilation, central metabolism, and oxidative tricarboxylic acid (TCA) cycle (in black); a reductive branch of TCA cycle (in blue); Sbm pathway (in purple); glyoxylate shunt (in light orange/brown). Metabolite abbreviations: DHAP, dihydroxyacetone phosphate; G3P, glycerol-3-phosphate; Gly, glyoxylate; PEP, phosphoenolpyruvate. Protein abbreviations: AceA, isocitrate lyase; AceB, malate synthase A; AceK, isocitrate dehydrogenase kinase/phosphatase; AckA, acetate kinase; AdhE, aldehyde-alcohol dehydrogenase; FrdABCD, fumarate reductase complex; FumB, fumarate hydratase class I, anaerobic; IclR, AceBAK operon repressor; IDH, isocitrate dehydrogenase; MDH, malate dehydrogenase; PckA, phosphoenolpyruvate carboxykinase; PPC, phosphoenolpyruvate carboxylase; Pta, phosphotransacetylase; Sbm, methylmalonyl-CoA mutase; SdhABCD, succinate dehydrogenase complex; SucAB, 2-oxoglutarate dehydrogenase; SucCD, succinyl coenzyme A synthetase; YgfG, (*R*)-methylmalonyl-CoA carboxylase; YgfH, propionyl-CoA: succinate-CoA-transferase [Color figure can be viewed at wileyonlinelibrary.com]

poly(3-hydroxybutyrate-*co*-3-hydroxyvalerate) (Srirangan, Liu, Tran et al., 2016). Given the successful demonstration of propionate biosynthesis in engineered *E. coli* (Akawi et al., 2015), technological limitations existed. As the Sbm pathway is not physiologically essential in *E. coli*, the intracellular level of propionyl-CoA often remains low, limiting propionate biosynthesis. In addition, propionate biosynthesis via the Sbm pathway in the propanologenic *E. coli* was conducted under a limited oxygen supply, such as microaerobic conditions, hindering cell growth and therefore culture performance. The major objective of this study is to tackle these metabolic issues limiting propionate biosynthesis.

The Sbm pathway diverts from the tricarboxylic acid (TCA) cycle at the node of succinyl-CoA. Hence, high-level propionate biosynthesis presumably relies on effective diversion of the carbon flux from the TCA cycle into the Sbm pathway. As propionate was synthesized under relatively anaerobic conditions, succinyl-CoA is derived from succinate via SucCD in the reductive (i.e., reverse) TCA direction. Hence, succinate becomes a plausible target for metabolic manipulation. However, as succinate is involved in the central metabolism in a complex manner and its formation can be mediated through multiple oxygen-dependent pathways, manipulation of the carbon flux around this C4 compound can be challenging. Herein, we targeted several TCA cycle genes encoding enzymes near the succinyl-CoA node for genetic manipulation to investigate how the TCA carbon flux gets diverted into the Sbm pathway. With such a mechanistic understanding of the relevant metabolic flows, we developed consolidated metabolic engineering and bioprocessing strategies to enhance such carbon flux redirection for high-level propionate biosynthesis while reducing byproduct acetate accumulation, thus demonstrating potential industrial applicability of the developed bioprocess.

## 2 | MATERIALS AND METHODS

### 2.1 | Bacterial strains and plasmids

Bacterial strains and deoxyribonucleic acid (DNA) primers used in this study are listed in Table 1. Genomic DNA from bacterial cells was isolated using the Blood & Tissue DNA Isolation Kit (Qiagen, Hilden, Germany). Standard recombinant DNA technologies were applied for molecular cloning (Miller, 1992). *Taq* DNA polymerase was obtained from New England Biolabs (Ipswich, MA). All synthesized oligonucleotides were obtained from Integrated DNA Technologies (Coralville, IA). The DNA sequencing was conducted by the Center for Applied Genomics at the Hospital for Sick Children (Toronto, Canada). *E. coli* BW25113 was the parental strain for the derivation of all mutant strains in this study, and *E. coli* DH5α was used as a host for molecular cloning.

**TABLE 1** *Escherichia coli* strains and oligonucleotides used in this study

| Name | Description, relevant genotype or primer sequence (5′→3′) | Source |
|---|---|---|
| *E. coli* host strains | | |
| DH5α | F−, *endA1*, *glnV44*, *thi-1*, *recA1*, *relA1*, *gyrA96*, *deoR*, *nupG* $\phi$*80d lacZ*Δ*acZd ladlacZYA – argF) U169*, *hsdR17(rK-mK+)*, *λ-* | Lab stock |
| BW25141 | F-, *Δ(araD-araB)567*, *ΔlacZ4787(::rrnB-3)*, *Δ(phoB-phoR)580*, *λ-*, *galU95*, *ΔuidA3::pir+*, *recA1*, *endA9 (del-ins)::FRT*, *rph-1*, *Δ(rhaD-rhaB)568*, *hsdR514* | Datsenko and Wanner (2000) |
| BW25113 | F-, *Δ(araD-araB)567*, *ΔlacZ4787(::rrnB-3)*, *λ-*, *rph-1*, *Δ(rhaD-rhaB)568*, *hsdR514* | Datsenko and Wanner (2000) |
| BWΔ*ldhA*-CTRL | BW25113 ldhA null mutant | Srirangan, Liu, Akawi et al. (2016); Srirangan et al. (2014) |
| CPC-Sbm | BWΔ*ldhA*, P*trc::sbm* (i.e., with the FRT-P*trc* cassette replacing the 204-bp upstream of the Sbm operon) | Akawi et al. (2015) |
| CPC-SbmΔ*frdB* | *frdB* null mutant of CPC-Sbm | This study |
| CPC-SbmΔ*aceA* | *aceA* null mutant of CPC-Sbm | This study |
| CPC-SbmΔ*sucD* | *sucD* null mutant of CPC-Sbm | This study |
| CPC-SbmΔ*sdhA* | *sdhA* null mutant of CPC-Sbm | This study |
| CPC-SbmΔ*iclR* | *iclR* null mutant of CPC-Sbm | This study |
| CPC-SbmΔ*frdB*Δ*aceA* | *frdB* and *aceA* null mutant of CPC-Sbm | This study |
| CPC-SbmΔ*sdhA*Δ*iclR* | *sdhA* and *iclR* null mutant of CPC-Sbm | This study |
| Primers | | |
| v-ldhA | GATAACGGAGATCGGGAATGATTAA; GGTTTAAAAGCGTCGATGTCCAGTA | Akawi et al. (2015) |
| v-sdhA | CTCTGCGTTCACCAAAGTGT; ACACACCTTCACGGCAGGAG | This study |
| v-iclR | GGTGGAATGAGATCTTGCGA; CCGACACGCTCAACCCAGAT | This study |
| c-frt | AGATTGCAGCATTACACGTCTTGAG; CCAGCTGCATTAATGAATCGGGCCATGGTCCATATGAATATCCTCC | Srirangan et al. (2014) |
| c-ptrc | CCGATTCATTAATGCAGCTGG; GGTCTGTTTCCTGTGTGAAATTGTTA | Srirangan, Liu, Akawi et al. (2016) |

Abbreviation: Sbm, sleeping beauty mutase.

The activation of the genomic Sbm operon to generate propanologenic *E. coli* CPC-Sbm was described previously (Srirangan et al., 2014). Knockouts of the genes, including *frdB* (encoding fumarate reductase iron-sulfur subunit, FrdB), *aceA* (encoding isocitrate lyase, AceA), *sucD* (encoding succinate-CoA ligase, SucD), *sdhA* (encoding succinate dehydrogenase complex flavoprotein subunit A, SdhA), and *iclR* (encoding transcriptional AceBAK operon repressor, IclR), were introduced into CPC-Sbm by P1 phage transduction (Miller, 1992) using the appropriate Keio Collection strains (Coli Genetic Stock Center, Yale University, New Haven, CT) as donors (Baba et al., 2006). To eliminate the cotransduced FRT-$Kn^R$-FRT cassette, the transductants were transformed with pCP20 (Cherepanov & Wackernagel, 1995), a temperature-sensitive plasmid expressing a flippase (Flp) recombinase. Upon Flp-mediated excision of the $Kn^R$ cassette, a single Flp recognition site (FRT "scar site") was generated. Plasmid pCP20 was then cured by growing cells at 42°C. The genotypes of derived knockout strains were confirmed by colony polymerase chain reaction using the appropriate verification primer sets listed in Table 1.

## 2.2 | Media and bacterial cell cultivation

All medium components were obtained from Sigma-Aldrich Co. (St. Louis, MO) except yeast extract and tryptone, which were obtained from BD Diagnostic Systems (Franklin Lakes, NJ). *E. coli* strains, stored as glycerol stocks at −80°C, were streaked on lysogeny broth (LB) agar plates and incubated at 37°C for 14–16 hr.

For shake-flask cultivations, single colonies were picked from LB plates to inoculate 30ml LB medium (10 g/L tryptone, 5 g/L yeast extract, and 5 g/L NaCl) in 125-ml conical flasks. The cultures were shaken at 37°C and 280 rpm in a rotary shaker (New Brunswick Scientific, NJ) and used as seed cultures to inoculate 220 ml LB media at 1% (vol/vol) in 1L conical flasks. This second seed culture was shaken at 37°C and 280 rpm until an optical density of 0.80 $OD_{600}$ was reached. Cells were then harvested by centrifugation at 9,000*g* and 20°C for 10 min and resuspended in 30-ml modified M9 production media. The suspended culture was transferred into a 125ml screwed cap or vented cap plastic production flasks and incubated at 30°C at 280 rpm in a rotary shaker. Unless otherwise specified, the modified M9 production medium contained 30 g/L glycerol, 3.0 g/L succinate, 5 g/L yeast extract, 10 mM $NaHCO_3$, 1 mM $MgCl_2$, 0.2 μM cyanocobalamin (vitamin B12), fifth dilution of M9 salts mix (33.9 g/L $Na_2HPO_4$, 15 g/L $KH_2PO_4$, 5 g/L $NH_4Cl$, 2.5 g/L NaCl), 1,000th dilution of Trace Metal Mix A5 (2.86 g/L $H_3BO_3$, 1.81 g/L $MnCl_2{\cdot}4H_2O$, 0.222 g/L $ZnSO_4{\cdot}7H_2O$, 0.39 g/L $Na_2MoO_4{\cdot}2H_2O$, 79 μg/L $CuSO_4{\cdot}5H_2O$, 49.4 μg/L $Co(NO_3)_2{\cdot}6H_2O$), and supplemented with 0.1 mM isopropyl β-D-1-thiogalactopyranoside (IPTG). All shake-flask cultivation experiments were performed in triplicate.

For bioreactor cultivations, single colonies were picked from LB plates to inoculate 30mL super broth (SB) medium (32 g/L tryptone, 20 g/L yeast extract, and 5 g/L NaCl) in 125 ml conical flasks. Overnight cultures were shaken at 37°C and 280 rpm in a rotary shaker (New Brunswick Scientific) and used as seed cultures to inoculate 220 ml SB media at 1% (vol/vol) in 1 L conical flasks. This second seed culture was shaken at 37°C and 280 rpm for 14–16 hr. Cells were then harvested by centrifugation at 9,000*g* and 20°C for 10 min and resuspended in 50 ml fresh LB media. The suspended culture was used to inoculate a 1 L stirred tank bioreactor (containing two Rushton radial flow disks as impellers; CelliGen 115; Eppendorf AG, Hamburg, Germany) at 30°C and 430 rpm. The semidefined production medium in the batch bioreactor contained 30 g/L glycerol, 0.23 g/L $K_2HPO_4$, 0.51 g/L $NH_4Cl$, 49.8 mg/L $MgCl_2$, 48.1 mg/L $K_2SO_4$, 1.52 mg/L $FeSO_4$, 0.055 mg/L $CaCl_2$, 2.93 g/L NaCl, 0.72 g/L tricine, 10 g/L yeast extract, 10 mM $NaHCO_3$, 0.2 μM cyanocobalamin (vitamin $B_{12}$) and 1,000th dilution (i.e., 1 ml/L) trace elements (2.86 g/L $H_3BO_3$, 1.81 g/L $MnCl_2{\cdot}4H_2O$, 0.222 g/L $ZnSO_4{\cdot}7H_2O$, 0.39 g/L $Na_2MoO_4{\cdot}2H_2O$, 79 μg/L $CuSO_4{\cdot}5H_2O$, 49.4 μg/L $Co(NO_3)_2{\cdot}6H_2O$; Neidhardt, Bloch, & Smith, 1974), and supplemented with 0.1 mM IPTG. For fed-batch cultivation, the production strain was first cultivated in a batch mode, as described above, followed by three feeding phases, in each of which approximately 15 g/L glycerol was supplemented for extended cultivation until complete glycerol dissimilation. Microaerobic and semiaerobic conditions were maintained by purging air into the headspace and bulk culture, respectively, at 0.1 vvm, designated as aeration level I (AL-I) and AL-II. Aerobic conditions were maintained by sparging air into the bulk culture at 1 vvm (AL-III) or 2–4 vvm (AL-IV). The pH of the production culture was maintained at 7.0 ± 0.1 with 30% (vol/vol) $NH_4OH$ and 15% (vol/vol) $H_3PO_4$.

## 2.3 | Analysis

Culture samples were appropriately diluted with 0.15 M saline solution for measuring cell density in $OD_{600}$ using a spectrophotometer (DU520; Beckman Coulter, Fullerton, CA). The cell-free medium was prepared by centrifugation of the culture sample at 9,000*g* for 5 min, followed by filter sterilization using a 0.2 μM syringe filter. Extracellular metabolites and glycerol were quantified using high-performance liquid chromatography (HPLC; LC-10AT, Shimadzu, Kyoto, Japan) with a refractive index detector (RID; RID-10A, Shimadzu, Kyoto, Japan) and a chromatographic column (Aminex HPX-87H; Bio-Rad Laboratories, CA). The HPLC column temperature was maintained at 35°C and the mobile phase was 5 mM $H_2SO_4$ (pH 2) running at 0.6 ml/min. The RID signal was acquired and processed by a data processing unit (Clarity Lite; DataApex, Prague, Czech Republic).

# 3 | RESULTS

## 3.1 | Effects of succinate supplementation and oxygenic condition on propionate biosynthesis

Using CPC-Sbm with the activated Sbm operon (Srirangan et al., 2014) as the control strain, we first investigated the effects of

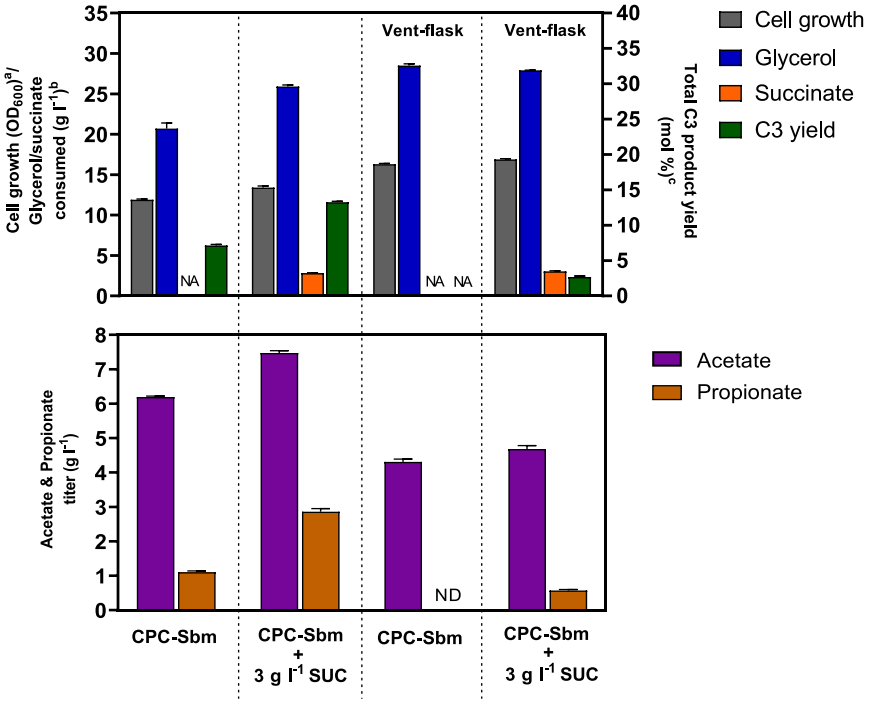


**FIGURE 2** Physiological effects of succinate supplementation and oxygenic conditions on propionate formation in shake-flask cultivation of CPC-Sbm. The top panel represents cell growth ($OD_{600}$), glycerol/succinate consumption, and C3 yield (%) whereas the bottom panel represents titers of acetate and propionate after 48 hr shake-flask cultivations. Unlabeled columns represent screw cap shake-flask cultivations. All values are reported as means ± *SD* (*n* = 3). Sbm, sleeping beauty mutase [Color figure can be viewed at wileyonlinelibrary.com]

succinate supplementation and oxygenic condition on propionate biosynthesis (Figure 2). Two types of shake flasks with either a screw cap (i.e., being more anaerobic) or vent cap (i.e., being more aerobic) were used to modulate the oxygenic condition of bacterial cultures. The screw cap shake-flask culture of CPC-Sbm with no succinate supplementation produced 1.1 g/L propionate with a C3 yield of 7.13%. Supplementing the screw cap shake-flask culture of CPC-Sbm with 3 g/L succinate resulted in a significant increase in propionate titer (2.86 g/L) with a nearly twofold of the C3 yield (13.3%) in comparison to the unsupplemented CPC-Sbm culture, suggesting that the metabolic activity of the Sbm pathway can be limited by succinate availability. However, C3 metabolites were hardly produced under more aerobic conditions in the vent cap shake-flask culture of CPC-Sbm, indicating that the metabolic activity of the Sbm pathway in the control strain CPC-Sbm was favored by anaerobic conditions. Interestingly, the effects of succinate supplementation were still observable under more aerobic culture conditions, with a trace amount of propionate (0.57 g/L) being detected in the vent cap shake-flask culture of CPC-Sbm supplemented with 3 g/L succinate.

## 3.2 | Metabolic routes in the TCA cycle leading to propionate biosynthesis

As the Sbm pathway diverts out of the TCA cycle via the succinyl-CoA node, it is critical to understand how the carbon flux gets redirected into the Sbm pathway for propionate biosynthesis. To do this, we knocked out several genes encoding enzymes near the succinyl-CoA node to observe their genetic effects on propionate biosynthesis (Figure 3; it should be noted that all cultivations were conducted in screw cap shake flasks except the last one.). These selective enzymes catalyze various critical reactions in the three major TCA routes toward succinate, that is, oxidative TCA cycle, reductive TCA branch, and glyoxylate shunt. Compared to the control strain CPC-Sbm, inactivation of the reductive TCA branch by mutating *frdB* in CPC-Sbm*Δfrd*B resulted in a notable reduction of propionate titer (0.79 g/L) and C3 yield (4.88%). However, inactivation of the glyoxylate shunt by mutating *aceA* in CPC-Sbm*ΔaceA* minimally affected propionate biosynthesis, with 1.18 g/L propionate and 7.95% C3 yield, compared to the control strain CPC-Sbm. Simultaneous inactivation of both the reductive TCA branch and glyoxylate shunt by mutating *frdB* and *aceA* in the double mutant CPC-Sbm*ΔfrdBΔaceA* further deteriorates, but insignificantly, propionate biosynthesis, compared with CPC-Sbm*ΔfrdB*. Furthermore, inactivation of the oxidative TCA cycle by mutating *sdhA* in CPC-Sbm*ΔsdhA* significantly improved propionate biosynthesis, with both the propionate titer (2.38 g/L) and C3 yield (15.17%) being approximately doubled in comparison to the control strain CPC-Sbm. Interestingly, the succinate/succinyl-CoA interconversion in the TCA cycle was determined essential for an operational Sbm pathway as mutating *sucD* in CPC-Sbm*ΔsucD* completely abolished propionate biosynthesis with a 0% C3 yield. These results suggest that, under the cultivation conditions in the screw cap shake-flask, the reductive TCA branch contributed a major portion of the carbon flux into the Sbm pathway for propionate biosynthesis in the control strain CPC-Sbm.

## 3.3 | Carbon flux redirection from the TCA cycle into the Sbm pathway

Normally, the glyoxylate shunt would be inactive as an expression of the key enzymes in this pathway, that is, AceBAK, is negatively

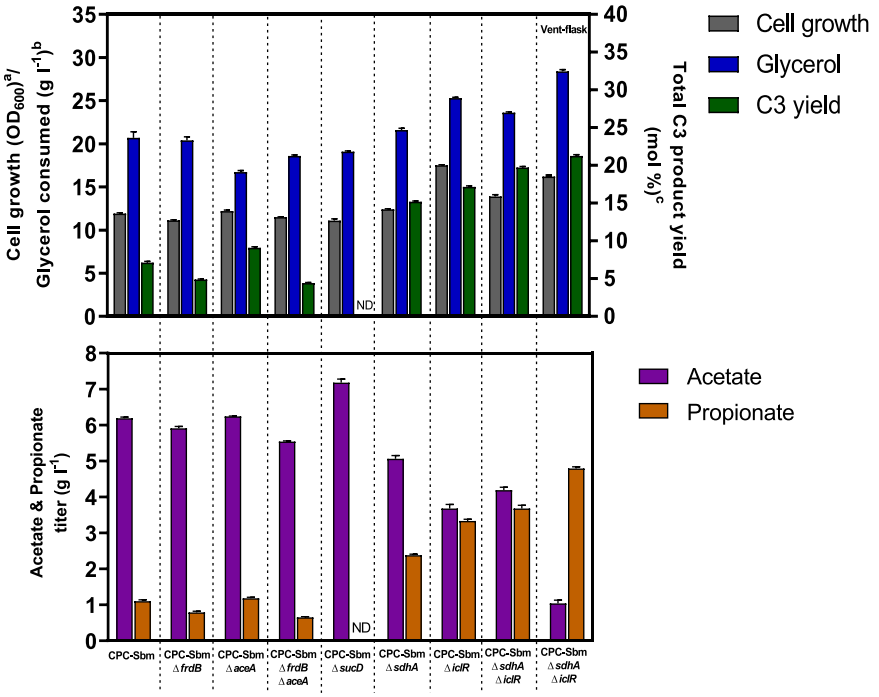


**FIGURE 3** Manipulation of TCA carbon flux by targeting several genes encoding enzymes near succinate node. The top panel represents cell growth ($OD_{600}$), glycerol consumption, and C3 yield (%) whereas the bottom panel represents titers of acetate and propionate reached after 48 hr shake-flask cultivations. Unlabeled columns represent screw cap shake-flask cultivations. All values are reported as means ± *SD* (*n* = 3). TCA, tricarboxylic acid [Color figure can be viewed at wileyonlinelibrary.com]

regulated by the IclR regulator. Deregulating the glyoxylate shunt by mutating *iclR* in CPC-SbmΔ*iclR* significantly improved propionate biosynthesis to 3.33 g/L, which was approximately threefold that of the control strain CPC-Sbm, with a much increased C3 yield to 17.1% and reduced acetate accumulation. Considering the two single mutants with significantly improved propionate biosynthesis, that is, CPC-SbmΔ*sdhA* and CPC-SbmΔ*iclR*, we derived a double mutant CPC-SbmΔ*sdhA*Δ*iclR* leading to a further increased propionate titer to 3.68 g/L and C3 yield to 19.7% in screw cap shake-flask cultures. Interestingly, cultivating CPC-SbmΔ*sdhA*Δ*iclR* under a more aerobic condition in vent cap shake flasks not only further improved propionate biosynthesis (4.79 g/L propionate and 21.3% C3 yield) but also drastically reduced acetate accumulation to 1.04 g/L, compared with 6.19 g/L acetate for the control strain CPC-Sbm in screw cap shake-flask cultures. The results suggest successful carbon flux redirection from the TCA cycle to the Sbm pathway for enhanced propionate biosynthesis in SbmΔ*sdhA*Δ*iclR* under cultivation conditions in the vent cap shake-flask.

## 3.4 | Batch cultivation in a bioreactor for propionate biosynthesis

As the oxygenic condition of the cultivation appeared to critically affect propionate biosynthesis and the oxygenic condition of a shake-flask culture could only be trivially modulated using either screw cap or vent cap, we further cultivated selective strains in a bioreactor with more defined aerobic/anaerobic levels. Using the control strain CPC-Sbm, bioreactor cultivation in a batch mode under three levels of aeration, that is, AL-I, AL-II, and AL-III from low to high was first used to characterize propionate biosynthesis (Figure 4). In general, the aeration level affected bacterial cultivation in terms of glycerol consumption (taking 35, 30, and 26 hr to consume 30 g/L glycerol under AL-I, AL-II, and AL-III, respectively), cell growth (final cell density reaching 17.4, 21.9, and 22.1 $OD_{600}$ under AL-I, AL-II, and AL-III, respectively), and acetate accumulation (final acetate titer reaching 9.32 g/L [45.3% acetate yield], 5.95 g/L [30.2% acetate yield], and 6.95 g/L [35.9% acetate yield] under AL-I, AL-II, and AL-III, respectively). In contrast, propionate biosynthesis was highly dependent on the oxygenic condition with the final propionate titer reaching 3.67 g/L (14.4% propionate yield), 1.81 g/L (7.43% propionate yield), 0 g/L (0% propionate yield) under AL-I, AL-II, and AL-III, respectively. These results were consistent with our shake-flask study and suggest that propionate biosynthesis in the control strain CPC-Sbm was favored under a low oxygenic condition.

In contrast, our shake-flask study showed that propionate biosynthesis in the double mutant CPC-SbmΔ*sdhA*Δ*iclR* was rather effective under a high oxygenic condition. Hence, we conducted three batches of bioreactor aerobic cultivation of CPC-SbmΔ*sdhA*, CPC-Sbm Δ*iclR*, and CPC-SbmΔ*sdhA*Δ*iclR* under AL-III (Figure 5). Compared with the control strain CPC-Sbm that produced no propionate under AL-III, mutating *sdhA* in CPC-SbmΔ*sdhA* led to defective carbon utilization (consuming only 19.8 g/L glycerol after 23 hr cultivation), poor cell growth (final cell density reaching only 13.8 $OD_{600}$), no propionate biosynthesis, and a high acetate accumulation (final acetate titer reaching 9.71 g/L accounting for 76.4% acetate yield) under AL-III. However, compared with the control strain CPC-Sbm under AL-III, inactivation of *iclR* in CPC-SbmΔ*iclR* hardly affected glycerol dissimilation, cell growth, and acetate accumulation of the culture, with an exception of producing 4.11 g/L propionate (17.0% propionate yield). The results suggest that activation of the glyoxylate shunt via the *iclR* mutation resulted

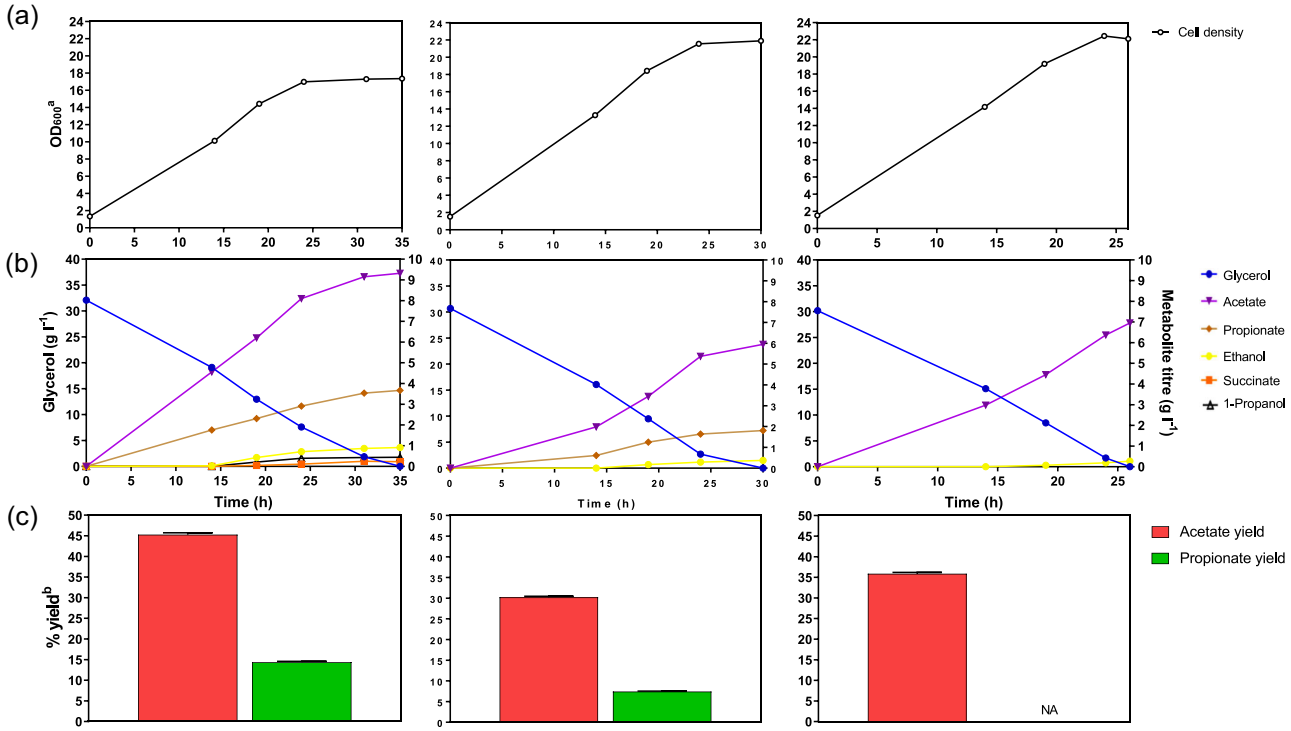


**FIGURE 4** Investigating the effects of varying aeration levels on propionate production in bioreactor cultivation of CPC-Sbm. Aeration conditions (from left to right): aeration level I (AL-I), aeration level II (AL-II), and aeration level III (AL-III). Time profiles of (a) cell growth ($OD_{600}$), (b) glycerol consumption and metabolite production, and (c) percentage of acetate/propionate metabolites theoretical yield based on consumed glycerol. All values are reported as means ± *SD* (*n* = 2). Sbm, sleeping beauty mutase [Color figure can be viewed at wileyonlinelibrary.com]

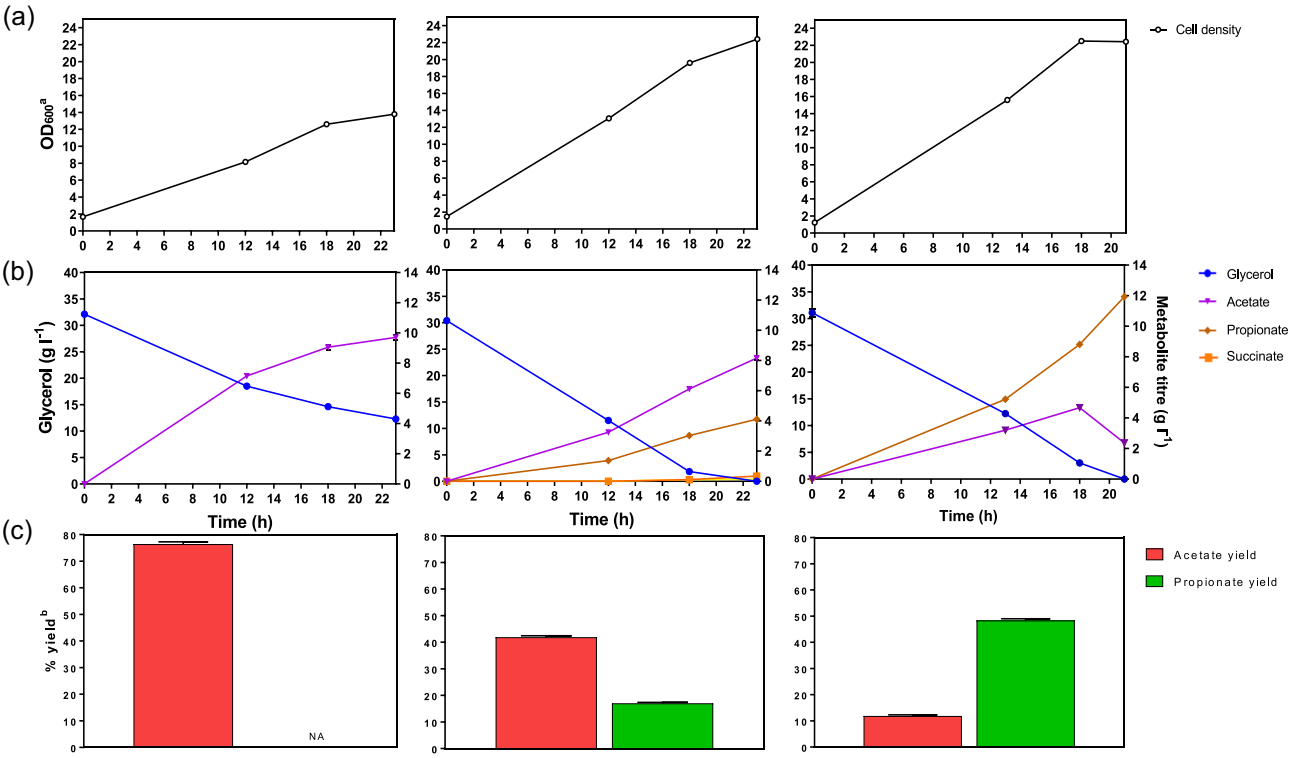


**FIGURE 5** Manipulation of the TCA cycle for propionate production under AL-III conditions. Strains tested (from left to right): CPC-SbmΔ*sdhA*, CPC-SbmΔ*iclR*, and CPC-SbmΔ*sdhA*Δ*iclR*. Time profiles of (a) cell growth ($OD_{600}$), (b) glycerol consumption and metabolite production, and (c) percentage of acetate/propionate metabolites theoretical yield based on consumed glycerol. All values are reported as means ± *SD* (*n* = 2). Sbm, sleeping beauty mutase; TCA, tricarboxylic acid [Color figure can be viewed at wileyonlinelibrary.com]

in more carbon flux redirection toward succinate and subsequently into the Sbm pathway, particularly under a high oxygenic condition. Propionate biosynthesis was significantly enhanced to 11.7 g/L (48.3% propionate yield) with a much-reduced acetate accumulation upon aerobic cultivation of the double mutant CPC-Sbm*ΔsdhAΔiclR* under AL-III, suggesting more effective carbon flux redirection into the Sbm pathway.

### 3.5 | Fed-batch cultivation for enhanced propionate biosynthesis

Using CPC-Sbm*ΔsdhAΔiclR*, we further conducted fed-batch cultivation by extending the existing batch with three pulse feedings, each at 15 g/L glycerol, under AL-III (Figure 6). In Feeding 1, cells continued to grow and the fed glycerol was effectively utilized for propionate biosynthesis with a high propionate yield of 60.2% and no acetate accumulation. In subsequent Feedings 2 and 3, the biosynthetic capacity of propionate steadily declined with propionate yields being reduced to 32.7% and 19.0%, respectively. The deteriorated propionate biosynthesis occurred with acetate over-accumulation to a final titer of 11.0 g/L, which could be associated with a limited oxygenic condition. Nevertheless, the AL-III fed-batch culture achieved a high final propionate titer of 26.8 g/L. To potentially minimize acetate accumulation, we conducted another fed-batch cultivation of CPC-Sbm*ΔsdhAΔiclR* under AL-IV by increasing the air purging rate to 2 vvm during the batch phase and to 4 vvm during the three feeding phases (Figure 7). In comparison to the AL-III fed-batch culture, the rates of cell growth and glycerol dissimilation for the AL-IV fed-batch culture slightly increased with a marginally reduced acetate accumulation, leading to a better propionate biosynthesis. A very high level of propionate biosynthesis

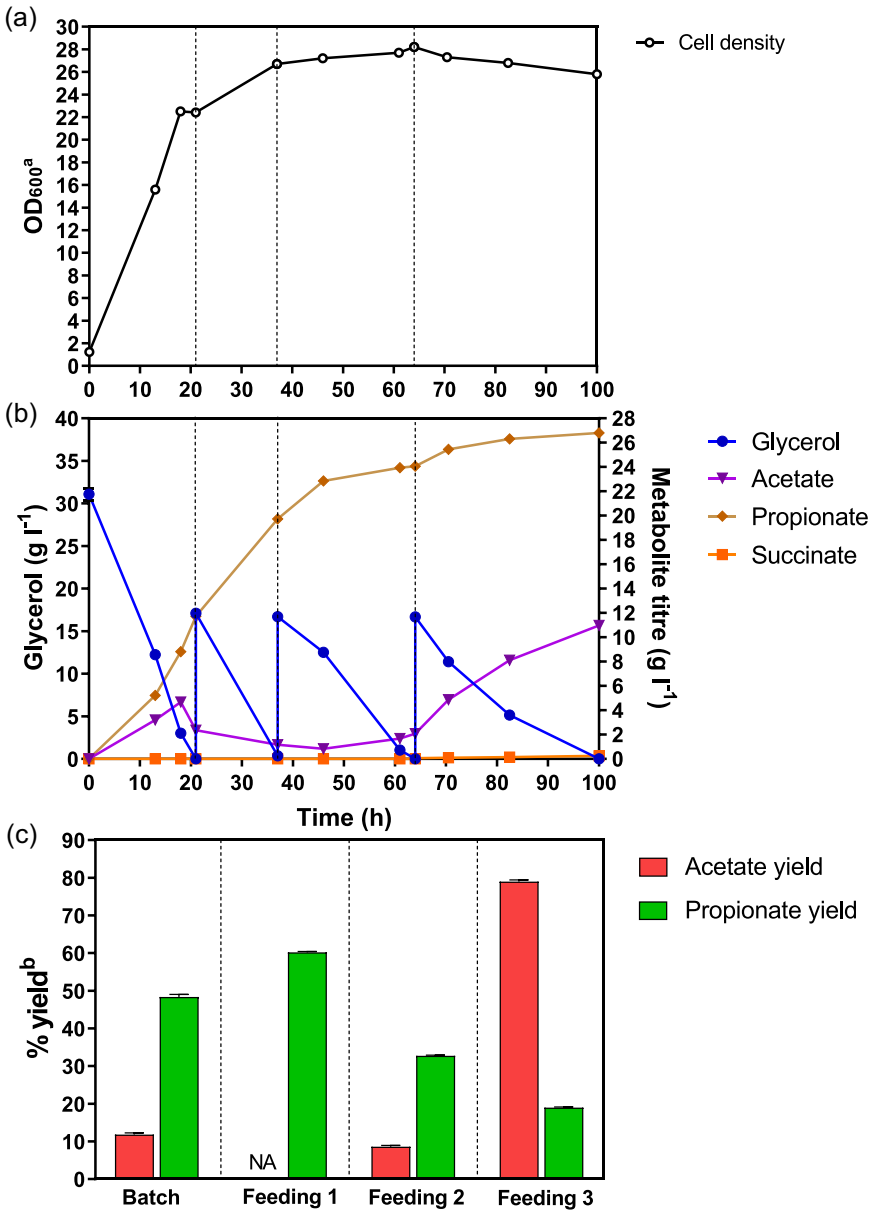


**FIGURE 6** Fed-batch cultivation of CPC-Sbm*ΔsdhAΔiclR* under extended AL-III conditions. Time profiles of (a) cell growth ($OD_{600}$), (b) glycerol consumption and metabolite production, and (c) percentage of acetate/propionate metabolites theoretical yield based on consumed glycerol during each feeding phase. Dotted vertical lines in panels a and b separate batch, Feeding 1, Feeding 2, and Feeding 3 stages of fermentation. All values are reported as means ± *SD* (*n* = 2). Sbm, sleeping beauty mutase [Color figure can be viewed at wileyonlinelibrary.com]

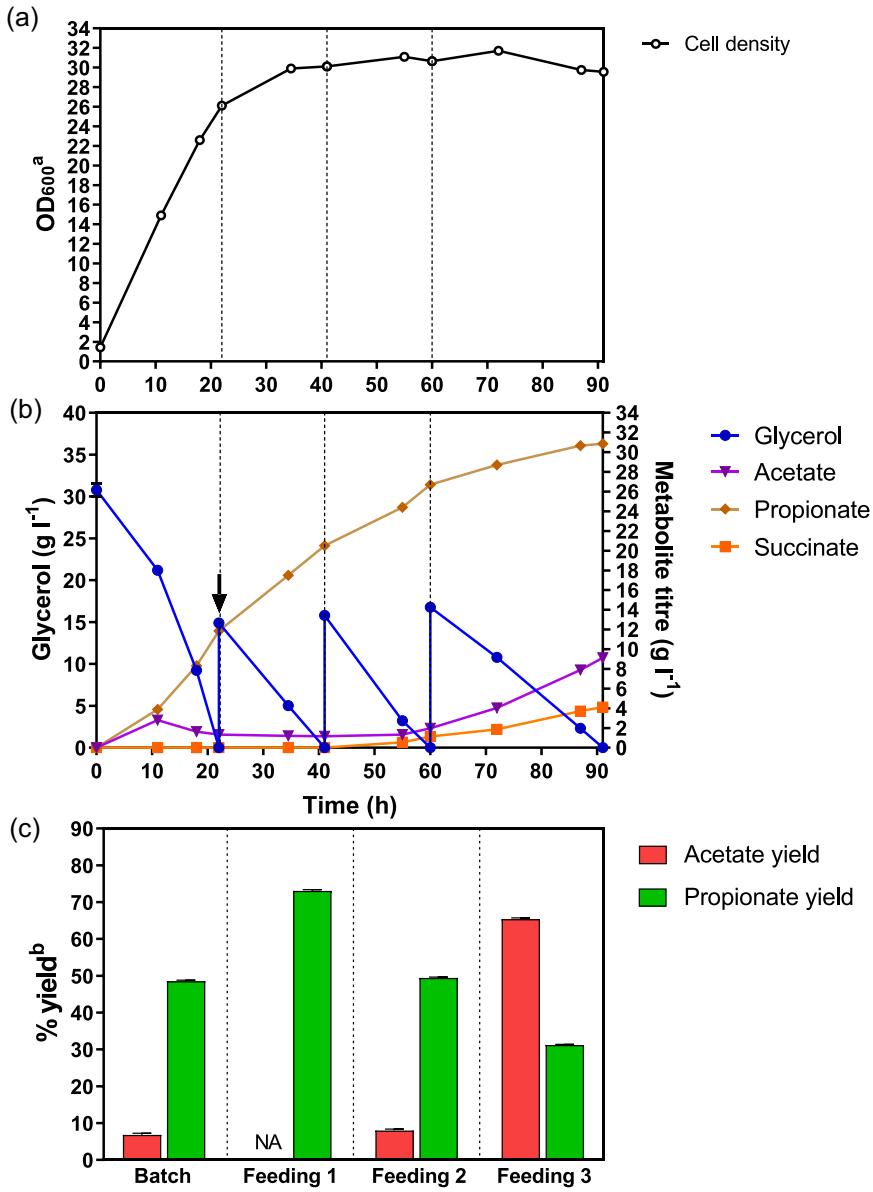


**FIGURE 7** Fed-batch cultivation of CPC-Sbm*ΔsdhAΔiclR* under AL-IV conditions. Time profiles of (a) cell growth ($OD_{600}$), (b) glycerol consumption and metabolite production, and (c) percentage of acetate/propionate metabolites theoretical yield based on consumed glycerol during each feeding phase. Dotted vertical lines in panels a and b separate batch, Feeding 1, Feeding 2, and Feeding 3 stages of fermentation. Black arrow indicates the point of airflow switch from 2 to 4 vvm. All values are reported as means ± *SD* ($n = 2$). Sbm, sleeping beauty mutase [Color figure can be viewed at wileyonlinelibrary.com]

with 73.1% propionate yield was also observed in Feeding 1 of the AL-IV fed-batch culture, whereas the subsequent Feedings 2 and 3, still showed a steady decline in propionate biosynthesis with propionate yields of 49.5% and 31.2%, respectively. It should be noted that the reduced acetate accumulation may have contributed to the enhanced propionate biosynthesis for the AL-IV fed-batch culture that achieved a high final propionate titer of 30.9 g/L with an overall propionate yield of 49.7%.

## 4 | DISCUSSION

As the results of succinate supplementation for the CPC-Sbm culture (Figure 2) suggest that propionate biosynthesis could be potentially limited by succinate availability, we derived several mutants by targeting selective TCA genes encoding enzymes near the succinyl-CoA node for manipulation to further understand how the carbon flux was diverted from the TCA cycle to the Sbm pathway. SucCD are TCA enzymes catalyze the interconversion of succinate and succinyl-CoA. Although mutating *sucCD* (encoding SucCD) can potentially disrupt the TCA cycle in both oxidative and reductive directions, *sucCD* are not essential genes as the physiologically required succinyl-CoA can still be derived via SucAB (Yu et al., 2006). However, succinyl-CoA derived from this half oxidative TCA branch cannot be funneled into the Sbm pathway as CPC-Sbm*ΔsucD* produced no propionate with 0% C3 yield, suggesting that both succinate availability and the conversion from succinate to succinyl-CoA in the reductive TCA branch were critical for carbon flux diversion into the Sbm pathway for propionate biosynthesis.

In *E. coli*, succinate is synthesized via three oxygen-dependent pathways in the TCA cycle, that is, (a) reductive TCA branch, (b) oxidative TCA cycle, and (c) glyoxylate shunt. Under anaerobic conditions, the dissimilated carbon from glycolysis enters the TCA cycle in the form of phosphoenolpyruvate (PEP), subjecting to

carboxylation to form oxaloacetate, and then proceeds with reactions in the reductive TCA branch to generate succinate as a final product (Cheng, Wang, Zeng, & Zhang, 2013). Although the reductive TCA branch can potentially yield high-level succinate, this pathway is generally unfavorable as it is limited by the availability of reducing equivalents (i.e., NADH; Skorokhodova, Morzhakova, Gulevich, & Debabov, 2015). However, under aerobic conditions, acetyl-CoA derived from glycolysis enters the oxidative TCA cycle to generate succinate as a cycle intermediate (Thakker, Martínez, San, & Bennett, 2012). In addition, under aerobic conditions, succinate can be generated alternatively via the glyoxylate shunt (Thakker et al., 2012), which is stimulated upon transcriptional activation of the *aceBAK* operon and negatively regulated by the IclR repressor (Nègre, Cortay, Galinier, Sauve, & Cozzone, 1992; Sunnarborg, Klumpp, Chung, & LaPorte, 1990). Hence, the glyoxylate shunt can be deregulated by mutating the repressor-encoded gene *iclR*. It should be noted that in *E. coli*, the glyoxylate shunt is operational under aerobic conditions (generating oxidative stresses) while consuming acetate or fatty acids (Cheng et al., 2013). Both the shake-flask (Figure 2) and bioreactor (Figure 4) results clearly show that propionate biosynthesis via the Sbm pathway in the control strain CPC-Sbm was favored by anaerobic conditions and was minimal under aerobic conditions, suggesting that the reductive TCA branch was the main carbon flux contributor toward the Sbm pathway. This claim was further corroborated by (a) minimally affected propionate biosynthesis and C3 yield upon inactivation of the glyoxylate shunt in CPC-SbmΔ*aceA*, (b) reduced propionate biosynthesis and C3 yield upon inactivation of the reductive TCA branch in CPC-SbmΔ*frdB*, and (c) significantly reduced propionate biosynthesis and C3 yield upon inactivation of both the reductive TCA branch and glyoxylate shunt in CPC-SbmΔ*frdB*Δ*aceA* (Figure 3). Finally, mutating *sucD* blocked the carbon flux toward succinyl-CoA via both the reductive TCA branch and glyoxylate shunt, and completely abolished propionate biosynthesis in CPC-SbmΔ*sucD*, further suggesting the critical role that SucD and its associated succinate-succinyl-CoA interconversion step played in the carbon flux redirection into the Sbm pathway.

Interestingly, but rather unexpectedly, inactivation of the oxidative TCA cycle significantly enhanced propionate biosynthesis and C3 yield in CPC-SbmΔ*sdhA* (Figure 3), presumably due to more active reductive TCA branch as the glyoxylate shunt was likely inactive under this genetic background and shake-flask culture conditions. The results of CPC-SbmΔ*sdhA*, along with the observations of literally no propionate biosynthesis under aerobic conditions in the control strain CPC-Sbm (Figures 2 and 4), suggest that the carbon flux contribution from the oxidative TCA cycle toward propionate biosynthesis was minimal. However, mutating *iclR* to deregulate glyoxylate shunt significantly enhanced propionate biosynthesis in CPC-SbmΔ*iclR* (Figure 3), suggesting that the glyoxylate shunt could be an alternative metabolic route contributing carbon flux toward the Sbm pathway. Combining the two mutations of Δ*sdhA* and Δ*iclR* could further drive the entire carbon flux arising from the glyoxylate shunt toward the Sbm pathway via the reductive TCA branch rather than the oxidative TCA cycle, further enhancing propionate biosynthesis in CPC-SbmΔ*sdhA*Δ*iclR* (Figure 3). The enhancement was even more pronounced when this double mutant was cultivated under higher aerobic conditions that stimulate the glyoxylate shunt.

While propionate biosynthesis in CPC-Sbm was favored by anaerobiosis under AL-I in a bioreactor, the low oxygenic level seriously retarded cell growth, resulting in acetate accumulation (Figure 4). The accumulation of acetate, derived from acetyl-CoA, could potentially limit dissimilated carbon flux from glycolysis toward the reductive TCA branch (at the PEP node) and then into the Sbm pathway (Figure 1). Although the retarded cell growth and acetate accumulation could be resolved by marginally increasing the oxygenic level through the cultivation of CPC-Sbm under AL-II (Figure 4), the resolution was at the expense of reduced propionate biosynthesis. Further increasing the oxygenic level to cultivate CPC-Sbm under AL-III completely abolished propionate biosynthesis, though cell growth was effective (Figure 4), implying that more dissimilated carbon flux upon glycolysis was directed toward the acetyl-CoA node to form acetate, rather than toward the PEP node into the reductive TCA branch and Sbm pathway.

The mutant strain CPC-SbmΔ*sdhA* with an inactivated TCA oxidative cycle had retarded cell growth with limited glycerol dissimilation and no propionate biosynthesis (Figure 5). Previous studies also showed that substantial inhibition of the TCA cycle under a high oxygen exposure upon disruption of the succinate dehydrogenase complex (encoded by *sdhABCD*) in *E. coli* resulted in reduced cell growth and metabolic activity (Guest, 1981; Steinsiek, Frixel, Stagge, & Bettenbrock, 2011). However, glyoxylate shunt could serve as an alternate route to drive the TCA cycle under aerobic conditions, and mutating *iclR* enhanced the metabolic activity of glyoxylate shunt, resulting in not only vigorous cell growth but also decent propionate biosynthesis in CPC-SbmΔ*iclR* under AL-III (Figure 5). The relatively low propionate yield was primarily associated with the still active TCA oxidative cycle in CPC-SbmΔ*iclR*, resulting in the diversion of the carbon flux arising from glyoxylate shunt at the succinate node to both oxidative and reductive TCA branches. Importantly, the flux diversion could be prevented by further blocking the oxidative TCA cycle such that the carbon flux was effectively redirected toward succinyl-CoA and then into the Sbm pathway in CPC-SbmΔ*sdhA*Δ*iclR* under AL-III (Figure 5). Such carbon flux redirection was ineffective when the oxidative TCA cycle was functional, resulting in reduced and even no propionate biosynthesis under AL-III in CPC-SbmΔ*iclR* (Figure 5) and CPC-Sbm (Figure 4), respectively. Also, it should be noted that the severely retarded glycerol dissimilation and cell growth for CPC-SbmΔ*sdhA* could be complemented by the *iclR* mutation, suggesting that both the oxidative TCA cycle and glyoxylate shunt contributed to active TCA operation for sustained cell growth under aerobic conditions. Finally, it should be noted that the issue of acetate accumulation was less severe for CPC-SbmΔ*iclR* and much improved for CPC-SbmΔ*sdhA*Δ*iclR*, suggesting that the enhanced glyoxylate shunt and disrupted oxidative TCA cycle could not only facilitate the carbon

flux redirection described above but also acetyl-CoA utilization, thereby reducing acetate formation. As the Sbm pathway was still active under AL-III for CPC-Sbm*ΔsdhAΔiclR*, the observation of no propionate biosynthesis in CPC-Sbm under AL-III was primarily associated with the shortage of succinate precursor for propionate biosynthesis.

Using the double mutant CPC-Sbm*ΔsdhAΔiclR*, we further demonstrated its excellent propionate-producing capacity through fed-batch cultivation under aerobic conditions of AL-III (Figure 6) and AL-IV (Figure 7), in particular, during certain feeding stages, such as Feeding 1 under AL-III and AL-IV, in which propionate biosynthesis was effective with high propionate yields of 60.2% and 73.1%, respectively, which are even comparable to those reached by natural producers (Gonzalez-Garcia et al., 2017). It should be noted that propionate biosynthesis was active throughout the three feeding phases of both fed-batch cultures. Nevertheless, the overall propionate production was limited by acetate accumulation, particularly during the Feedings 2 and 3 phases in the AL-III fed-batch culture. Such carbon spill issue was shown to be associated with oxygen limitation as increasing the aeration rate in the AL-IV fed-batch culture could moderately reduce acetate accumulation with further enhanced propionate biosynthesis, achieving a high final propionate titer at 30.9 g/L, which is the highest reported for *E. coli* thus far, with an overall propionate yield of 49.7%. It should be further noted that increasing the culture aerobicity can potentially enable cells to recycle the accumulated acetyl-CoA (thereby reduce acetate accumulation) for biosynthesis through enhanced glyoxylate shunt, which involves acetyl-CoA as a cosubstrate and is typically active under aerobic conditions (Ahn, Jung, Jang, Madsen, & Park, 2016; Renilla et al., 2012). Hence, our results suggest that the Sbm pathway can be metabolically active under both anaerobic and aerobic conditions. The molecular and metabolic engineering approaches presented in this study are potentially applicable to the bio-based production of other chemicals derived from succinyl-CoA.

## ACKNOWLEDGMENTS

This study was supported by the following Government of Canada grants: (a) Natural Sciences and Engineering Research Council (NSERC) Strategic Partnership grant 430106-12; (b) Canada Research Chair (CRC) grant 950-211471; and (c) Networks of Centers of Excellence of Canada (BioFuelNet Canada [BFN]).

## CONFLICT OF INTERESTS

The authors declare that there are no conflict of interests.

## AUTHOR CONTRIBUTIONS

D. M. conceived the study, formulated the research plan, coordinated the research team, carried out experiments, performed result interpretation and data analysis, and drafted the manuscript. J.-Y. M. helped to carry out experiments. M.-M. Y. and C. P. C. conceived, planned, supervised, and managed the study, as well as helped to draft the manuscript. All authors read and approved the final manuscript.

## ORCID

*Chih-Hsiung Perry Chou* http://orcid.org/0000-0002-7254-8118

## REFERENCES

Ahmadi, N., Khosravi-Darani, K., & Mortazavian, A. M. (2017). An overview of biotechnological production of propionic acid: From upstream to downstream processes. *Electronic Journal of Biotechnology*, *28*, 67–75.

Ahn, S., Jung, J., Jang, I. -A., Madsen, E. L., & Park, W. (2016). Role of glyoxylate shunt in oxidative stress response. *Journal of Biological Chemistry*, *291*(22), 11928–11938.

Akawi, L., Srirangan, K., Liu, X., Moo-Young, M., & Chou, C. P. (2015). Engineering *Escherichia coli* for high-level production of propionate. *Journal of Industrial Microbiology & Biotechnology*, *42*(7), 1057–1072.

Baba, T., Ara, T., Hasegawa, M., Takai, Y., Okumura, Y., Baba, M., … Mori, H. (2006). Construction of *Escherichia coli* K-12 in-frame, single-gene knockout mutants: The Keio collection. *Molecular Systems Biology*, *2*, 1–11.

Chen, G.-Q. (2009). Industrial production of PHA, *Plastics from Bacteria* (pp. 121–132). New York: Springer.

Cheng, K.-K., Wang, G.-Y., Zeng, J., & Zhang, J.-A. (2013). Improved succinate production by metabolic engineering. *BioMed Research International*, *2013*, 538790.

Cherepanov, P. P., & Wackernagel, W. (1995). Gene disruption in *Escherichia coli*: $Tc^R$ and $Km^R$ cassettes with the option of Flp-catalyzed excision of the antibiotic-resistance determinant. *Gene*, *158*(1), 9–14.

Cho, C., Choi, S. Y., Luo, Z. W., & Lee, S. Y. (2015). Recent advances in microbial production of fuels and chemicals using tools and strategies of systems metabolic engineering. *Biotechnology Advances*, *33*(7), 1455–1466.

Datsenko, K. A., & Wanner, B. L. (2000). One-step inactivation of chromosomal genes in *Escherichia coli* K-12 using PCR products. *Proceedings of the National Academy of Sciences of the United States of America*, *97*, 6640–6645.

Fabbri, P., Viaggi, D., Cavani, F., Bertin, L., Michetti, M., Carnevale, E., … Marscheider-Weidemann, F. (2018). Ecologic Institute 2018: Top emerging bio-based products, their properties and industrial applications. *Ecologic Institute*, 1–28.

Gonzalez-Garcia, R. A., McCubbin, T., Navone, L., Stowers, C., Nielsen, L. K., & Marcellin, E. (2017). Microbial propionic acid production. *Fermentation*, *3*(2), 1–21.

Guest, J. R. (1981). Partial replacement of succinate dehydrogenase function by phage- and plasmid-specified fumarate reductase in *Escherichia coli*. *Journal of General Microbiology*, *122*(2), 171–179.

Ikeda, M. (2003). Amino acid production processes. In R. Faurie, J. Thommel, B. Bathe, V. G. Debabov, S. Huebner, M. Ikeda & W. Pfefferle (Eds.), *Microbial production of L-amino acids* (pp. 1–35). Berlin, Germany: Springer.

Miller, J. H. (1992). *A short course in bacterial genetics: a laboratory manual and handbook for* Escherichia coli *and related bacteria* (pp. 1–876). New York, NY: Cold Spring Harbor Laboratory Press.

Nègre, D., Cortay, J. -C., Galinier, A., Sauve, P., & Cozzone, A. J. (1992). Specific interactions between the IclR repressor of the acetate operon of *Escherichia coli* and its operator. *Journal of Molecular Biology*, *228*(1), 23–29.

Neidhardt, F. C., Bloch, P. L., & Smith, D. F. (1974). Culture medium for enterobacteria. *Journal of Bacteriology*, *119*(3), 736–747.

Renilla, S., Bernal, V., Fuhrer, T., Castaño-Cerezo, S., Pastor, J. M., Iborra, J. L., … Cánovas, M. (2012). Acetate scavenging activity in *Escherichia coli*: Interplay of acetyl–CoA synthetase and the PEP–glyoxylate cycle in chemostat cultures. *Applied Microbiology and Biotechnology*, *93*(5), 2109–2124.

Show, P. L., Oladele, K. O., Siew, Q. Y., Aziz-Zakry, F. A., Lan, J. C. -W., & Ling, T. C. (2015). Overview of citric acid production from *Aspergillus niger*. *Frontiers in Life Science*, *8*(3), 271–283.

Skorokhodova, A. Y., Morzhakova, A. A., Gulevich, A. Y., & Debabov, V. G. (2015). Manipulating pyruvate to acetyl-CoA conversion in *Escherichia coli* for anaerobic succinate biosynthesis from glucose with the yield close to the stoichiometric maximum. *Journal of Biotechnology*, *214*, 33–42.

Srirangan, K., Akawi, L., Liu, X., Westbrook, A., Blondeel, E. J. M., Aucoin, M. G., … Chou, C. P. (2013). Manipulating the sleeping beauty mutase operon for the production of 1-propanol in engineered *Escherichia coli*. *Biotechnology for Biofuels*, *6*, 1–14.

Srirangan, K., Liu, X., Akawi, L., Bruder, M., Moo-Young, M., & Chou, C. P. (2016). Engineering *Escherichia coli* for microbial production of butanone. *Applied and Environmental Microbiology*, *82*, 2574–2584.

Srirangan, K., Liu, X., Tran, T. T., Charles, T. C., Moo-Young, M., & Chou, C. P. (2016). Engineering of *Escherichia coli* for direct and modulated biosynthesis of poly(3-hydroxybutyrate-*co*-3-hydroxyvalerate) copolymer using unrelated carbon sources. *Scientific Reports*, *6*, 36470.

Srirangan, K., Liu, X., Westbrook, A., Akawi, L., Pyne, M. E., Moo-Young, M., & Chou, C. P. (2014). Biochemical, genetic, and metabolic engineering strategies to enhance coproduction of 1-propanol and ethanol in engineered *Escherichia coli*. *Applied Microbiology and Biotechnology*, *98*(22), 9499–9515.

Steinsiek, S., Frixel, S., Stagge, S., & Bettenbrock, K. (2011). Characterization of *E. coli* MG1655 and *frdA* and *sdhC* mutants at various aerobiosis levels. *Journal of Biotechnology*, *154*(1), 35–45.

Sunnarborg, A., Klumpp, D., Chung, T., & LaPorte, D. C. (1990). Regulation of the glyoxylate bypass operon: Cloning and characterization of *iclR*. *Journal of Bacteriology*, *172*(5), 2642–2649.

Thakker, C., Martínez, I., San, K. Y., & Bennett, G. N. (2012). Succinate production in *Escherichia coli*. *Biotechnology Journal*, *7*(2), 213–224.

Yu, B. J., Sung, B. H., Lee, J. Y., Son, S. H., Kim, M. S., & Kim, S. C. (2006). *sucAB* and *sucCD* are mutually essential genes in *Escherichia coli*. *FEMS Microbiology Letters*, *254*(2), 245–250.

**How to cite this article:** Miscevic D, Mao J-Y, Moo-Young M, Chou CP. High-level heterologous production of propionate in engineered *Escherichia coli*. *Biotechnology and Bioengineering*. 2020;117:1304–1315. https://doi.org/10.1002/bit.27276